Arch. Mech., **69**, 3, pp. 257–267, Warszawa 2017

# Translational and rotational Brownian displacements of colloidal particles of complex shapes

B. CICHOCKI[1)], M. L. EKIEL-JEŻEWSKA[2)], E. WAJNRYB[2)]

[1)] *Institute of Theoretical Physics*
*Faculty of Physics*
*University of Warsaw*
*Pasteura 5*
*02-093 Warsaw, Poland*

[2)] *Institute of Fundamental Technological Research*
*Polish Academy of Sciences*
*Pawińskiego 5B*
*02-106 Warsaw, Poland*
*e-mail: mekiel@ippt.pan.pl*

The exact analytical expressions for the time-dependent cross-correlations of the translational and rotational Brownian displacements of a particle with arbitrary shape were derived by us in [3, 4]. They are in this work applied to construct a method to analyze the Brownian motion of a particle of an arbitrary shape, and to extract accurately the self-diffusion matrix from the measurements of the cross-correlations, which in turn allows to gain some information on the particle structure. As an example, we apply our new method to analyze the experimental results of D. J. Kraft *et al.* for the micrometer-sized aggregates of the beads [8]. We explicitly demonstrate that our procedure, based on the measurements of the time-dependent cross-correlations in the whole range of times, allows to determine the self-diffusion (or alternatively the friction matrix) with a much higher precision than the method based only on their initial slopes. Therefore, the analytical time-dependence of the cross-correlations serves as a useful tool to extract information about particle structure from trajectory measurements.

**Key words:** Brownian motion, Smoluchowski equation, hydrodynamic interactions, self-diffusion matrix, friction coefficients, cross-correlations of translational and rotational Brownian displacements.



## 1. Introduction

The characteristic time scales of the translational and rotational Brownian diffusion for nanoparticles are typically much smaller than the time resolution of experiments. In this case, nanoparticles can be treated as point-like, and described by the standard Brownian theory [1]. However, for microparticles, the characteristic Brownian time scales are of the order of seconds, and therefore non-negligible in comparison to the typical time scales of the measured Brownian motion. For

microparticles of complex shapes, a more general theoretical approach is needed to account for the time-dependent Brownian translational and rotational displacements and their cross-correlations. Such an approach has been recently developed, and new analytical expressions have been derived from the Smoluchowski equation for the Brownian motion of a particle with an arbitrary shape [2–4].

Nowadays, there is a lot of interest in experimental studies of Brownian particles of relatively large sizes [5–8]. Therefore, it seems useful to demonstrate explicitly how to apply the theoretical scheme from [3, 4] to analyze the data from measurements. In this work, we use the interesting experiment from [8] as the reference for such a comparison. In [8], the Brownian motions of symmetric and non-symmetric microparticles were investigated at time scales comparable with the characteristic time of the rotational Brownian diffusion. The time-dependent cross-correlations of the Brownian translational and orientational displacements of microparticles with different shapes were measured and the initial slopes of these curves were used to experimentally determine the friction matrices. Based on the details of the particle shape, known from the experiment, these matrices were also evaluated numerically with HYDROSUB [9], and then used as the input to time-dependent numerical simulations of the Brownian displacement cross-correlations. Qualitatively, the results agree with each other, but there are significant quantitative differences, which the authors explain were due to by the statistical uncertainty of the measurements and irregularities in the actual particle shapes.

In this paper, we look at the results in [8] from a more general perspective. If similar measurements are performed for a particle of unknown shape, how can the experimental data be used to extract as much details of the particle structure as possible? This information is contained in the mobility matrix (or, equivalently, its inverse called the friction matrix). Therefore, the key point is to construct such a theoretical scheme that allows to determine from the experiments the mobility coefficients (and therefore some information on the particle structure) with the best possible precision. The analytical expressions from [3, 4] serve this purpose: they can be used to fit the friction (or, equivalently, mobility) coefficients of a particle using its Brownian displacement cross-correlations in the whole range of the measured times. This procedure allows to determine experimentally the mobility coefficients (and therefore a more detailed structure of the particle) with a significantly higher precision than taking into account only the initial slope of the correlation functions, as in [8].

## 2. Goals and theoretical framework

It is worthwhile to consider two generic cases.

Case 1, analyzed in Section 3. The particle structure and size are known and the goal is to study its translational and rotational Brownian motion.

Case 2, described in Section 4. The particle structure is not known, and the Brownian displacement cross-correlations are used to determine its mobility coefficients which in turn provide information about the particle structure and size.

Numerical computations performed in [8] correspond to the first case. However, analysis of experimental data is often related to the second case. The challenging question is if the cross-correlations measurements can be analyzed with a precision high enough to provide information about the particle geometry.

In this paper, we apply the analytic expressions from [3, 4] to satisfy both goals. In Section 3, we perform calculations that belong to the first case. In Section 4, we generalize this approach to the second case.

The basic theoretical framework used in Section 3 is as follows. First, we evaluate the mobility matrix $\boldsymbol{\mu}$, which, by definition, gives the particle translational and rotational velocities when multiplied by the hydrodynamic force and torque exerted by the particles on the fluid [3, 10]. We do it for the particles at their initial orientations. The inverse of $\boldsymbol{\mu}$, called the friction matrix, is denoted as $\eta\boldsymbol{\mathcal{H}}$, as in [8],

$$\eta\boldsymbol{\mathcal{H}} = \boldsymbol{\mu}^{-1}. \tag{2.1}$$

Therefore, the translational-translational, rotational-translational and rotational-rotational elements of $\boldsymbol{\mathcal{H}}$ are given in terms of $\mu$m, $\mu$m$^2$ and $\mu$m$^3$, respectively.

We also evaluate the diffusion tensor $\boldsymbol{\mathcal{D}}$, with all the translational-translational, rotational-translational and rotational-rotational parts,

$$\boldsymbol{\mathcal{D}} = \begin{bmatrix} \boldsymbol{D}^{tt} & \boldsymbol{D}^{tr} \\ \boldsymbol{D}^{rt} & \boldsymbol{D}^{rr} \end{bmatrix}, \tag{2.2}$$

for the particles at their initial orientations,

$$\boldsymbol{\mathcal{D}} = k_B T \boldsymbol{\mu}, \tag{2.3}$$

where $k_B$ is the Boltzmann constant and $T$ is the temperature.

Next, we use the elements of the diffusion matrix $\boldsymbol{\mathcal{D}}$ to determine the cross-correlation matrix $\mathbf{C}(t)$ of the time-dependent Brownian translational and orientational displacements of these particles [3, 4]

$$\mathbf{C}(t) = \begin{bmatrix} \langle \Delta\mathbf{R}(t)\Delta\mathbf{R}(t)\rangle_0 & \langle \Delta\mathbf{R}(t)\Delta\mathbf{u}(t)\rangle_0 \\ \langle \Delta\mathbf{u}(t)\Delta\mathbf{R}(t)\rangle_0 & \langle \Delta\mathbf{u}(t)\,\Delta\mathbf{u}(t)\rangle_0 \end{bmatrix}, \tag{2.4}$$

with $\Delta\mathbf{R}$ and $\Delta\mathbf{u}(t)$ defined as in [3, 4, 8],

$$\Delta\mathbf{R}(t) = \mathbf{R}(t) - \mathbf{R}(0), \tag{2.5}$$

$$\Delta\mathbf{u}(t) = \frac{1}{2}\sum_{p=1}^{3} \mathbf{u}^{(p)}(0) \times \mathbf{u}^{(p)}(t), \tag{2.6}$$

where $\mathbf{R}(t)$ denotes the time-dependent position of a reference center and $\mathbf{u}^{(p)}(t)$, $p = 1, 2, 3$, are three mutually perpendicular unit vectors describing the particle orientation at time $t$ [3, 8].

The initial slope of the cross-correlation matrix is related to the diffusion matrix $\boldsymbol{\mathcal{D}}$,

$$\left.\frac{d\mathbf{C}(t)}{dt}\right|_{t=0} = 2\boldsymbol{\mathcal{D}}. \tag{2.7}$$

The averages $\langle \ldots \rangle_0$ are taken with respect to the particle positions and orientations, using the conditional probability which satisfies the Smoluchowski equation [1, 11].

To determine the hydrodynamic friction matrix $\eta\boldsymbol{\mathcal{H}}$ and the diffusion tensor $\boldsymbol{\mathcal{D}}$ for a given particle (case 1), we solve the Stokes equations, supplemented by the boundary conditions at the particle surface, using the multipole method with the lubrication correction, implemented in the accurate numerical codes HYDROMULTIPOLE [12]. We apply the multipole truncation order $L = 20$. Then, we apply the expressions for the cross-correlations derived from the Smoluchowski equation in [3, 4].

For spheres or some other symmetric particle shapes, the mobility and friction matrices are diagonal. Therefore, the mobility center [10] coincides with the center of mass, we are in the frame in which the rotational-rotational diffusion tensor is diagonal, and we can directly use the simple analytical expressions derived in [3]. For irregular shapes, we first rotate the system of coordinates to the reference frame in which the rotational-rotational diffusion matrix is diagonal. Still, the translational-rotational coupling does not vanish, and therefore, we use more complicated analytical expressions for the cross-correlations from [4]. To compare with the experiments, we rotate back the frame of reference to the one shown in Fig. 1.

In Section 3, this procedure (case 1) will be applied to an experimental example. Section 4 considers the backward case 2, where the correlations are known (experimentally) but the mobility matrix is not.

## 3. Case 1: Calculations

### 3.1. Particles

Following [8], we consider three particles: regular trimer, regular tetramer and irregular trimer, made of spheres (labeled by $i = 1, 2, 3, 4$). For the regular trimer and regular tetramer, the beads have equal diameters $d$ and overlap, with equal distances $l$ between the closest bead centers, with $d = 2.1$ μm and $l = 1.5$ μm for the trimer and $d = 2.4$ μm and $l = 2.3$ μm for the tetramer. For the irregular

trimer, the beads have diameters $d_1 = 2.1$ μm, $d_2 = 1.3$ μm, $d_3 = 1.7$ μm, they do not overlap, and the distances between the bead centers are $l_{13} = 2.2$ μm,

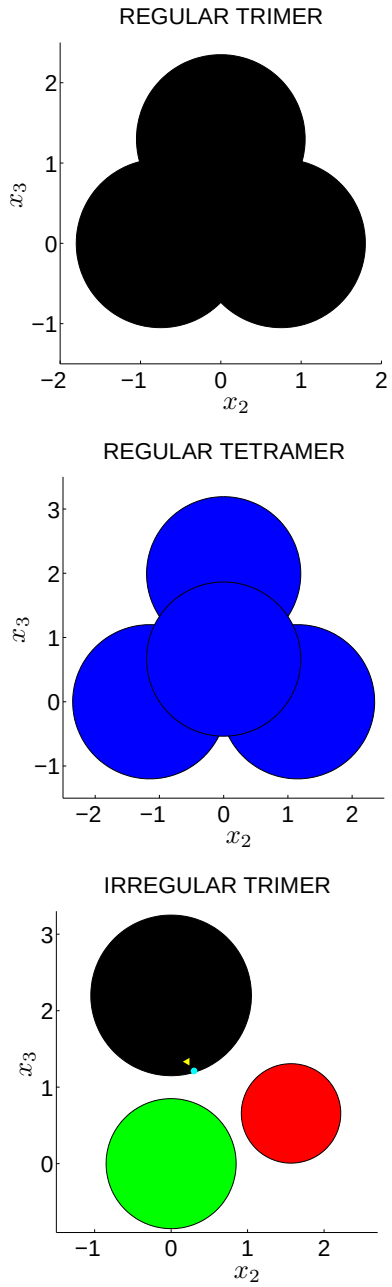


FIG. 1. Bead models of different rigid particles. For irregular trimer, the center of mass (yellow triangle) does not coincide with the mobility center (cyan circle).

$l_{12} = 2.2$ μm, $l_{23} = 1.7$ μm. The particles at their initial orientations with respect to the chosen coordinate system are shown in Fig. 1; the centers of three beads are in the plane $x_1 = 0$. From now on we will choose the center of mass position as the reference center position $\mathbf{R}(t)$, and will use the same notation as in [8], to allow for the comparison with the experiments.

### 3.2. Fluid

In [8], the fluid dynamic viscosity was $\eta = 2.22$ mPa s and the temperature $T = 294$ K. With these values, time is expressed in seconds and denoted as $t$.

### 3.3. Regular trimer

For the regular trimer at the chosen orientation shown in Fig. 1, the friction matrix has the form

$$\boldsymbol{\mathcal{H}} = \begin{pmatrix} 30.5 & 0 & 0 & 0 & 0 & 0 \\ 0 & 28.4 & 0 & 0 & 0 & 0 \\ 0 & 0 & 28.4 & 0 & 0 & 0 \\ 0 & 0 & 0 & 112 & 0 & 0 \\ 0 & 0 & 0 & 0 & 89.3 & 0 \\ 0 & 0 & 0 & 0 & 0 & 89.3 \end{pmatrix}, \tag{3.1}$$

with the units of $\mathcal{H}_{ii}$ equal to $\mu$m for $i = 1, 2, 3$ and $\mu$m$^3$ for $i = 3, 4, 5$.

The cross-correlations are given by the same expressions as for axially symmetric shapes [3]:

$$C_{11} = 0.126\,t - 0.0481(1 - e^{-0.123\,t}), \tag{3.2}$$

$$C_{22} = C_{33} = 0.126\,t + 0.0240(1 - e^{-0.123\,t}), \tag{3.3}$$

$$C_{44} = \tfrac{1}{6} + \tfrac{1}{12}e^{-0.123\,t} - \tfrac{1}{2}e^{-0.106\,t} + \tfrac{1}{4}e^{-0.0410\,t}, \tag{3.4}$$

$$C_{55} = C_{66} = \tfrac{1}{6} - \tfrac{1}{6}e^{-0.123\,t} - \tfrac{1}{4}e^{-0.119\,t} + \tfrac{1}{4}e^{-0.0367\,t}, \tag{3.5}$$

where $t$ denotes time in seconds, and the units of $C_{ii}$ are equal to μm$^2$ for $i = 1, 2, 3$ and are dimensionless for $i = 3, 4, 5$.

The expressions (3.2)–(3.5) are plotted versus time in seconds in the top row of Fig. 2. The off-diagonal components vanish.

### 3.4. Regular tetramer

For the regular tetramer at the chosen orientation shown in Fig. 1, the friction matrix has the form:

$$\boldsymbol{\mathcal{H}} = \begin{pmatrix} 39.7 & 0 & 0 & 0 & 0 & 0 \\ 0 & 39.7 & 0 & 0 & 0 & 0 \\ 0 & 0 & 39.7 & 0 & 0 & 0 \\ 0 & 0 & 0 & 248 & 0 & 0 \\ 0 & 0 & 0 & 0 & 248 & 0 \\ 0 & 0 & 0 & 0 & 0 & 248 \end{pmatrix}, \tag{3.6}$$

with the units of $\mathcal{H}_{ii}$ equal to $\mu$m for $i = 1, 2, 3$ and $\mu\text{m}^3$ for $i = 3, 4, 5$.

The cross-correlations are given by the same expressions as for a spherical particle [3]:

$$C_{11} = C_{22} = C_{33} = 0.0920\, t, \tag{3.7}$$

$$C_{44} = C_{55} = C_{66} = \frac{1}{6} - \frac{5}{12} e^{-0.0443\, t} + \frac{1}{4} e^{-0.0148\, t}, \tag{3.8}$$

where $t$ denotes time in seconds. The expressions (3.7)–(3.8) are plotted versus time in the middle row of Fig. 2. The off-diagonal components vanish.

### 3.5. Irregular trimer

For the irregular trimer at the chosen orientation shown in Fig. 1, the friction matrix has the form:

$$\boldsymbol{\mathcal{H}} = \begin{pmatrix} 29.9 & 0 & 0 & 0 & -4.06 & -2.95 \\ 0 & 28.0 & 0.318 & 2.92 & 0 & 0 \\ 0 & 0.318 & 26.6 & 2.07 & 0 & 0 \\ 0 & 2.92 & 2.07 & 117 & 0 & 0 \\ -4.06 & 0 & 0 & 0 & 101 & 8.51 \\ -2.95 & 0 & 0 & 0 & 8.51 & 69.3 \end{pmatrix}, \tag{3.9}$$

with the units of $\mathcal{H}_{ij}$ equal to $\mu$m for $i, j = 1, 2, 3$ and $\mu\text{m}^3$ for $i, j = 3, 4, 5$ and $\mu\text{m}^2$ for the t-r and r-t coefficients.

To determine the cross-correlations, we first go to the frame of reference where the rotational-rotational part of the mobility matrix is diagonal, and evaluate the correlation matrix $\mathbf{C}^{diag}$ in this frame, using the explicit expressions from [4]. Then, with the use of the $3 \times 3$ transformation matrix $\boldsymbol{T}$, we transform it to the original frame of reference,

$$C_{n+i,m+l} = T_{ij}^{-1} C_{n+j,m+k}^{diag} T_{lk}. \tag{3.10}$$

In Eq. (3.10), $i, j, k, l = 1, 2, 3$ are the Cartesian components, and $n, m = 0, 3$ label the translational and rotational parts of the correlation matrix. The expressions are lengthy and therefore not explicitly written in this note. All the non-vanishing translational-translational, translational-rotational and rotational-rotational correlations are plotted in the bottom row of Fig. 2.

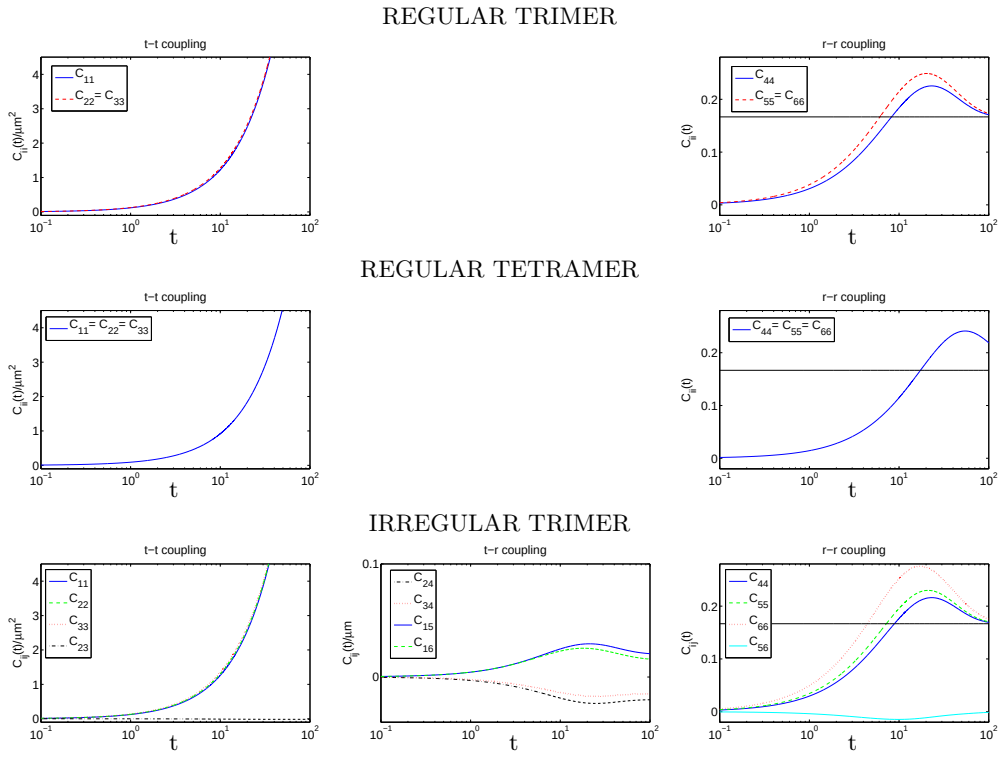


FIG. 2. Cross-correlations $C_{ij}(t)$ for regular trimer (top row), regular tetramer (middle row) and irregular trimer (bottom row). Translational-translational, translational-rotational and rotational-rotational couplings are shown in the left, middle and right columns, respectively. Horizontal line: $C_{44}(\infty) = C_{55}(\infty) = C_{66}(\infty) = 1/6$. Here, $t$ denotes time in seconds.

### 3.6. Discussion

In general, the numerical friction tensors and cross-correlations of the Brownian displacements presented in [8] agree well with our results presented in this paper. No wonder, since they are obtained for the same sizes and relative positions of the spherical beads that model the particle shape. The only meaningful differences are observed the rotational-translational couplings of the irregular trimer which are small and difficult to be determined numerically. Comparing the corresponding elements of the hydrodynamic friction matrices in Eqs. (3.1), (3.6) and (3.9) with those given in Fig. 1 of [8], we need to take into account different geometries and accuracies of the models. In the HYDROSUB algorithm and numerical program, used in [8], the surface of the particle is represented by a shell of small elements ("minibeads"); the results are extrapolated to a zero minibead radius [9]. In this work, each sphere of the cluster is represented by a single bead, and the accurate HYDROMULTIPOLE numerical codes based on

a very precise multipole method corrected for lubrication are used to evaluate the friction matrix elements [12].

## 4. Case 2: new method

We will now apply our analytical expressions from [4] to analyze the experimental results for the irregular trimer given in [8]. For this particle, the non-linear deviations present in the analytical expressions from Section 3.5 are very small, and the theoretical translational-translational correlations grow with time almost linearly. We will now estimate the corresponding self-diffusion constant that characterizes the isotropic mean square displacement at large times. According to the results of [2], for times much longer that the characteristic scales of the rotational self-diffusion, the mean square displacement is a linear function of time, with the slope that does not depend on the choice of a reference point, and is equal to $6D_{cm}$, where $D_{cm}$ is the translational self-diffusion coefficient for the center of mobility. The center of mobility is such a reference point for which the translational-rotational mobility matrix is symmetric [10]. The explicit expression for $D_{cm}$ (see Eq. (20) in [4]) reads:

$$D_{cm} = \frac{1}{3}\left[\operatorname{Tr} \boldsymbol{D}^{tt} - \sum_{\alpha=1}^{3} \frac{(D^{rt}_{\beta\gamma} - D^{rt}_{\gamma\beta})^2}{D_\beta + D_\gamma}\right], \tag{4.1}$$

where $(\alpha, \beta, \gamma)$ is a permutation of $(1, 2, 3)$, Tr stands for the trace operation, and $D_\mu$ are the rotational-rotational diffusion coefficients, defined in the frame of reference in which $\boldsymbol{D}^{rr}$ is diagonal, i.e.

$$D^{rr}_{\mu\nu} = D_\mu \delta_{\mu\nu}, \tag{4.2}$$

with $\mu, \nu = 1, 2, 3$.

Using the theoretical and experimental friction matrices, we obtain $D_{cm} = 0.065$ $\mu\text{m}^2/\text{s}$ and $0.073$ $\mu\text{m}^2/\text{s}$, respectively. However, the experimental results shown in Fig. 2 in [8] correspond to value of $D_{cm}$ which is around two times smaller. There is a clear mismatch between the values that characterize essential feature of the Brownian motion: the value deduced from the measured time-dependent translational-translational correlations in a wide range of times and the value determined from the initial slopes of these functions. This difference can be understood by taking into account large statistical uncertainty of the experimental results. However, there is no doubt that a method based on fitting $C(t)$ in the whole range of times is more accurate than the method based on the initial slope.

Therefore, we propose the following new method to determine the self-diffusion matrix $\boldsymbol{\mathcal{D}}$ from the measured time-dependent cross-correlation matrix $\mathbf{C}(\mathbf{t})$.

First, we determine (and go to) the frame of reference in which the matrix $\langle \Delta\mathbf{u}(t)\,\Delta\mathbf{u}(t)\rangle_0$ is diagonal. Then, we use the time-dependent analytic expressions from [4] to determine in this frame $D_1$, $D_2$, $D_3$, and the rest of the self-diffusion coefficients. Finally, we can transform $\boldsymbol{\mathcal{D}}$ back to the original frame of reference. This procedure can be applied to particles of arbitrary shapes.

## 5. Conclusions

Summarizing, in this paper we have demonstrated the applicability of the new method, using the recent experimental results of [8] as an illuminating example. Even if the particles from [8] have only a small difference between the center of mobility and center of mass it is worth further emphasizing that the described procedure works for general particles tracking from an arbitrary tracking point.

It is very typical for experimentalists to use the initial slope of the cross-correlations of the Brownian translational and rotational displacements (as in Eq. (2) from [8]) to determine the diffusion matrix. However, the new method proposed here is based on the full fit of the cross-correlations $C(t)$ in the whole range of time when the measurements have been performed. Therefore, it is much more accurate.

## Acknowledgments

M.L.E.-J. was supported in part by the Polish National Science Centre (Narodowe Centrum Nauki) under Grant No. 2014/15/B/ST8/04359.

## References

1. N. van Kampen, *Stochastic Processes in Physics and Chemistry*, 3rd ed., North-Holland, 2007.
2. B. Cichocki, M.L. Ekiel-Jeżewska, E. Wajnryb, *Communication: translational Brownian motion for particles of arbitrary shape*, J. Chem. Phys., **136**, 071102-1-4, 2012.
3. B. Cichocki, M.L. Ekiel-Jeżewska, E. Wajnryb, *Brownian motion of a particle with arbitrary shape*, J. Chem. Phys., **142**, 214902-1-16, 2015.
4. B. Cichocki, M.L. Ekiel-Jeżewska, E. Wajnryb, *Note: Brownian motion of colloidal particles of arbitrary shape*, J. Chem. Phys., **144**, 076101-1-2, 2016.
5. A. Chakrabarty, A. Konya, F. Wang, J.V. Selinger, K. Sun, Q.-H. Wei, *Brownian motion of arbitrary shaped particles in two dimensions*, Langmuir, **30**, 13844–13853, 2014.
6. A. Wang, T.G. Dicasemiduk, J. Fung, S. Razavi, I. Kretzschmar, K. Chaudhary, V.N. Manoharan, *Using the discrete dipole approximation and holographic microscopy to measyre rotational dynamics of non-spherical colloidal particles*, J. Quant. Spectrosc. Radiat. Transfer, **146**, 499–509, 2014.

7. L. KOENS, E. LAUGA, *The passive diffusion of Leptospira interrogans*, Phys. Biol., **11**, 066008, p. 12, 2014.

8. D.J. KRAFT, R. WITTKOWSKI, B. TEN HAGEN, K.V. EDMOND, D.J. PINE, H. LÖWEN, *Brownian motion and the hydrodynamic friction tensor for colloidal particles of complex shape*, Phys. Rev. *E*, **88**, 050301, 2013.

9. J. GARCIA DE LA TORRE, B. CARRASCO, *Hydrodynamic properties of rigid macromolecules composed of ellipsoidal and cyryndrical subunits*, Biopolimers **63**, 3, 163–167, 2002; see also: J.G. DE LA TORRE, *The HYDRO suite of programs for rigid-particle hydrodynamics*, leonardo.inf.um.es/macromol/programs/hydrosuite.pdf.

10. S. KIM, S.J. KARRILA, *Microhydrodynamics: Principles and Selected Applications*, Butterworth-Heinemann, Boston, 1991.

11. R.B. JONES, P.N. PUSEY, *Dynamics of suspended colloidal spheres*, Annu. Rev. Phys. Chem., **42**, 137–169, 1991.

12. B. CICHOCKI, M.L. EKIEL-JEŻEWSKA, E. WAJNRYB, *Lubrication corrections for three-particle contribution to short-time self-diffusion coefficients in colloidal dispersions*, J. Chem. Phys., **111**, 3265 (1999).

*Received October 20, 2016; revised version January 30, 2017.*